Spatial and temporal patterns of ERK signaling during mouse embryogenesis

Laura Beth Corson[1], Yojiro Yamanaka[1], Ka-Man Venus Lai[1,2,*] and Janet Rossant[1,2,†]

[1]Samuel Lunenfeld Research Institute, Mount Sinai Hospital, Toronto, ON, Canada
[2]Department of Molecular and Medical Genetics, University of Toronto, ON, Canada
*Present address: Regeneron Pharmaceuticals, Tarrytown, NY, USA
†Author for correspondence (e-mail: rossant@mshri.on.ca)

Accepted 9 June 2003

Development 130, 4527-4537

doi:10.1242/dev.00669

Summary

Signaling between tissues is essential to form the complex, three-dimensional organization of an embryo. Because many receptor tyrosine kinases signal through the RAS-MAPK pathway, phosphorylated ERK can be used as an indicator of when and where signaling is active during development. Using whole-mount immunohistochemistry with antibodies specific to phosphorylated ERK1 and ERK2, we analyzed the location, timing, distribution, duration and intensity of ERK signaling during mouse embryogenesis (5-10.5 days postcoitum). Spatial and temporal domains of ERK activation were discrete with well-defined boundaries, indicating specific regulation of signaling in vivo. Prominent, sustained domains of ERK activation were seen in the ectoplacental cone, extraembryonic ectoderm, limb buds, branchial arches, frontonasal process, forebrain, midbrain-hindbrain boundary, tailbud, foregut and liver. Transient activation was seen in neural crest, peripheral nervous system, nascent blood vessels, and anlagen of the eye, ear and heart. In the contiguous domains of ERK signaling, phospho-ERK staining was cytoplasmic with no sign of nuclear translocation. With few exceptions, the strongest domains of ERK activation correlated with regions of known or suspected fibroblast growth factor (FGF) signaling, and brief incubation with an inhibitor of the fibroblast growth factor receptor (FGFR) specifically diminished the phospho-ERK staining in these regions. Although many domains of ERK activation were FGFR-dependent, not all domains of FGF signaling were phospho-ERK positive. These studies identify key domains of sustained ERK signaling in the intact mouse embryo, give significant insight into the regulation of this signaling in vivo and pinpoint regions where downstream target genes can be sought.

Key words: Mouse, Embryo, MAPK, ERK, FGF Signaling

Introduction

Signaling between tissues is essential for shaping the three-dimensional organization of the mouse embryo. Numerous developmental processes are mediated by growth factors signaling through receptor tyrosine kinases (RTKs). Ligands bind to the extracellular domains of transmembrane RTKs causing receptor dimerization, autophosphorylation and activation of the intracellular tyrosine kinase domains. This, in turn, leads to the activation of a number of intracellular signaling cascades, including the RAS-MAPK pathway (Marshall, 1995; Schlessinger, 2000). RTK activation leads to RAS activation which, in turn, induces sequential phosphorylation of the protein kinases RAF, MEK and ERK (MAPK). Activated ERK induces a variety of downstream responses including gene transcription, translation and cytoskeletal rearrangement. This RTK-RAS-MAPK pathway is moderated, at various points, by negative feedback regulators, including Sproutys, MAP kinase phosphatases, Spred and RasGAP (Feldmann et al., 1999; Furthauer et al., 2002; Tefft et al., 2002; Wakioka et al., 2001).

Although this RAS-MAPK pathway is not the only signaling cascade downstream of RTKs, it is often the key pathway for many RTK-mediated cell fate decisions. For example, in *C. elegans* and *D. melanogaster*, mutations in ERK genes often give rise to phenotypes similar to those generated by a loss of the RTKs themselves, and defects in various RTK signaling pathways can be compensated by gain-of-function alleles of RAS, RAF, MEK and/or ERK (Marshall, 1995). In vertebrates, numerous gain- and loss-of-function experiments have implicated RTK signaling in various developmental processes, including gastrulation, vasculogenesis, limb development, neural patterning and placentation. Although these studies reveal general roles of fibroblast growth factor (FGF), epidermal growth factor (EGF), vascular endothelial growth factor (VEGF) and neurotrophin signaling in specific developmental events, they do not reveal the precise location and timing of the signaling interactions that occur during the genesis of the tissue or structure. Although the expression domains of receptors and ligands identify potential regions of signaling, they cannot reveal when ligands begin actively signaling, the direction and distance across which ligands act, or the intensity and duration of signaling. In order to view

actual domains of RTK signaling, a direct readout of RTK activation is needed.

Whole-mount immunohistochemistry with antibodies specific to the di-phosphorylated forms of ERK1 and ERK2 (dp-ERK) has been used to map active ERK signaling domains within *Drosophila*, *Xenopus* and zebrafish embryos (Christen and Slack, 1999; Curran and Grainger, 2000; Gabay et al., 1997a; Gabay et al., 1997b; Reich et al., 1999; Sawada et al., 2001; Shinya et al., 2001). Although other pathways, such as integrins, cytokines and G-protein-coupled-receptors, can activate the RAS-MAPK pathway (Belcheva and Coscia, 2002; Widmann et al., 1999), the majority of dp-ERK domains correspond to RTK signaling domains in these embryos. Dp-ERK patterns are discrete and dynamic in embryos and correlate largely with regions of FGF and EGF signaling. These studies have given significant insight into RTK-MAPK signaling events guiding various developmental processes in these species. Limited analysis of mouse embryos indicated this approach would be feasible in the analysis of mouse embryogenesis as well (Lai and Pawson, 2000).

In this study, we have used whole-mount immunohistochemistry with phospho-ERK antibodies to map the spatial and temporal patterns of ERK activation during early postimplantation mouse development. In many cases, dp-ERK detection has enabled us to determine the timing, duration and intensity of receptor activation, to visualize gradients and boundaries of activation and to postulate the distribution of active ligand. This atlas of dp-ERK domains provides insight into how RTK signaling (FGF signaling in particular) is shaping the mouse embryo and how this signaling is regulated in vivo, and pinpoints regions where downstream target genes can be sought.

Materials and methods

Immunohistochemistry

Embryos were obtained from natural matings of ICR mice at different stages of gestation. The embryos were dissected rapidly in ice-cold PBS and transferred immediately to cold fixative to preserve endogenous dp-ERK signaling patterns. A detailed protocol for staining whole-mount mouse embryos with phosphorylation-specific antibodies can be found at http://www.mshri.on.ca/rossant/protocols.html. Briefly, embryos were fixed in 8% paraformaldehyde overnight, dehydrated in methanol, bleached with 5% H_2O_2, rehydrated, blocked with FBS-TBST (5% sera in TBS + 0.1% Triton), incubated with primary antibody overnight (in FBS-TBST), washed six times (1 hour each), incubated with biotinylated secondary antibody overnight, washed six times, and incubated with either fluorophore-conjugated streptavidin or with Vectastain HRP-avidin-biotin complex (Vector Laboratories).

Primary antibodies

Two different primary antibodies against the diphosphorylated forms of ERK1 and ERK2 as well as a primary antibody against total ERK1 and ERK2 (Cell Signaling Technology) were used in this study. The first phospho-ERK antibody was a mouse monoclonal antibody (#M8159, Sigma) raised against a synthetic diphosphorylated peptide corresponding to highly conserved residues around Thr183/Tyr185 of ERK2. This antibody has been widely used to map dp-ERK domains in *Drosophila*, *Xenopus* and zebrafish embryos (Christen and Slack, 1999; Curran and Grainger, 2000; Gabay et al., 1997a; Gabay et al., 1997b; Reich et al., 1999; Sawada et al., 2001; Shinya et al., 2001). The second phospho-ERK antibody was a rabbit polyclonal antibody raised against a similar (if not identical) peptide (#9101, Cell Signaling Technology). The two antibodies gave essentially the same staining patterns in mouse except in regions where endogenous mouse immunoglobulins reside. Mouse monoclonal antibody staining is problematic in such regions owing to the crossreactivity of secondary anti-mouse antibodies to the endogenous immunoglobulins found in the tissue. For this reason, the rabbit polyclonal antibody was used in the majority of these studies.

Secondary antibodies

Detection methods included biotinylated secondary antibodies (Jackson ImmunoResearch Laboratories) in conjunction with either Cy3-streptavidin (Jackson ImmunoResearch Laboratories) or Vectastain HRP ABC Reagent (Vector Laboratories). Because the HRP reaction catalyzed the formation of a precipitate that could diffuse from the position of the primary antibody, fluorophore-conjugated streptavidin gave better resolution of antigen location. To visualize nuclei in fluorophore-labeled embryos, embryos were incubated in Hoechst 33342 or YOYO-1 (Molecular Probes).

Sectioning

After imaging, whole-mount DAB-stained embryos were embedded in paraffin wax, cut into 10 μm sections and counterstained with Toluidine Blue. Whole-mount embryos labeled with Cy3 were sectioned transversely (~50 μm sections) with glass needles and mounted in 80% glycerol between coverslips.

Imaging

Smaller whole-mount embryos (<8.0 dpc) were photographed on a DMIRBE compound microscope (Leica) with DIC optics and standard epifluorescence using a CCD camera (Hamamatsu) and Openlab software (Improvision). Larger whole-mount embryos were imaged on a MZFLIII stereoscope (Leica) with liquid crystal filter (CRI) and the Hamamatsu-Openlab imaging system.

For higher resolution, a Zeiss LSM510 confocal or Delta Vision Olympus deconvolution system was used. For confocal imaging, the pinhole was set wider than 1 Airy unit and a series of thicker (~5 μm) optical sections were taken. In some instances, all the serial sections have been overlaid, using the Zeiss confocal software, to give a composite confocal image. In other instances, a single confocal section is presented.

Embryo culture

In order to verify that staining was specific to the phosphorylated form of ERK and to determine which domains of dp-ERK staining were specifically due to FGFR signaling, embryos were briefly treated with chemical inhibitors to MAPK kinase (U0126, Cell Signaling Technology) or to FGFR (SU5402, CalBiochem) prior to dp-ERK staining. Embryos were dissected out of the deciduas and placed in 1-2 ml of RPMI with 1% BSA, pre-equilibrated at 37°C, 5% CO_2. A final concentration of 0.1% DMSO was added to each culture. Controls contained DMSO only and experimental cultures included 50 μM U0126 (dissolved in DMSO) or 40 μM SU5402 (dissolved in DMSO). It was determined empirically that smaller embryos required ~30 minutes for the inhibitors to penetrate and mediate a response while larger embryos required up to 90 minutes. Cultures were rotated gently every 10 minutes during the incubation period at 37°C, 5% CO_2.

Results

Specificity of phosphorylated-ERK staining in mouse embryos

To visualize ERK signaling patterns during mouse development, embryos were stained with antibodies specific for the diphosphorylated forms of ERK1 and ERK2 (dp-ERK). Two different phosphorylation-specific ERK antibodies gave

essentially the same discrete patterns, while an antibody to total ERK protein gave ubiquitous staining (not shown). This indicated that although the ERK protein was widely expressed, the regions of ERK phosphorylation and hence regions of active ERK signaling were restricted. To further confirm the specificity of staining for the phosphorylated form of ERK, embryos were incubated with a MEK inhibitor (U0126), which specifically blocks the MAPK kinases (MEK1 and MEK2) responsible for phosphorylation of ERK1 and ERK2. As seen in Fig. 1K,L, dp-ERK staining diminished significantly in embryos treated with the MEK inhibitor. Taken together, this provided strong evidence that the regions of positive dp-ERK staining were indeed the domains of active ERK signaling in the mouse embryo.

Overview of ERK signaling in the postimplantation mouse embryo

Shown in Fig. 1 are representative dp-ERK patterns in postimplantation embryos. At all stages of development, contiguous, discrete domains of activated ERK were apparent, as well as weaker, scattered dp-ERK staining. Some domains were consistently positive for dp-ERK staining over periods of 2-3 days, suggestive of sustained RTK signaling, while other regions showed more transient ERK activation. A more detailed description of the specific domains is given below.

5.0-8.0 dpc

The most intense, sustained dp-ERK domains in 5-8 dpc embryos were in extra-embryonic tissues. Dp-ERK staining was first observed throughout the extra-embryonic ectoderm (Exe) at ~5.5 dpc (Fig. 1B) and then became restricted to a ring in the most proximal region of the Exe in subsequent days (Fig. 1C-F). The intensity of this dp-ERK domain as well as the cellular depth of the band decreased from 6 to 8 dpc and was barely detectable after 8.0 dpc. In the ectoplacental cone (EPC), ERK signaling began throughout the EPC shortly after EPC formation (~5.5 dpc) and was sustained in the central, diploid population of EPC cells in subsequent days (6-8 dpc) (Fig. 1B-F).

In contrast to these regions of sustained signaling that were readily detectable in every embryo, there were also regions of dp-ERK staining which were not observed in all embryos isolated at a given stage (±0.5 dpc). These seem to represent areas of signaling confined to a narrow window of development. Such dynamic regions of ERK signaling were found in the distal tip of the epiblast (~5.5 dpc) (Fig. 1B), the allantoic bud (~7.5 dpc) (Fig. 1D), blood island mesoderm (~7.5 dpc) (Fig. 1D), headfold mesoderm (Fig. 1E) and heart primordia (early headfold to 4-somite) (Fig. 1F). Scattered dp-ERK staining was seen in mitotic cells in some regions of embryonic ectoderm and mesoderm throughout development (see Fig. 1B-D). No significant dp-ERK staining was associated with the primitive streak or newly forming somites at any stage of development.

8.0-10.5 dpc

As the complexity of the embryo increased so too did the complexity of the dp-ERK patterns. The most prominent and consistently reproducible domains of sustained signaling were the frontonasal process (9.0-10.5+ dpc), forebrain (8.5-10+ dpc), midbrain-hindbrain boundary (8.5-10.5 dpc), branchial arches (9.0-10.5+ dpc), foregut (8.5-9.0 dpc), limb buds (9.0-

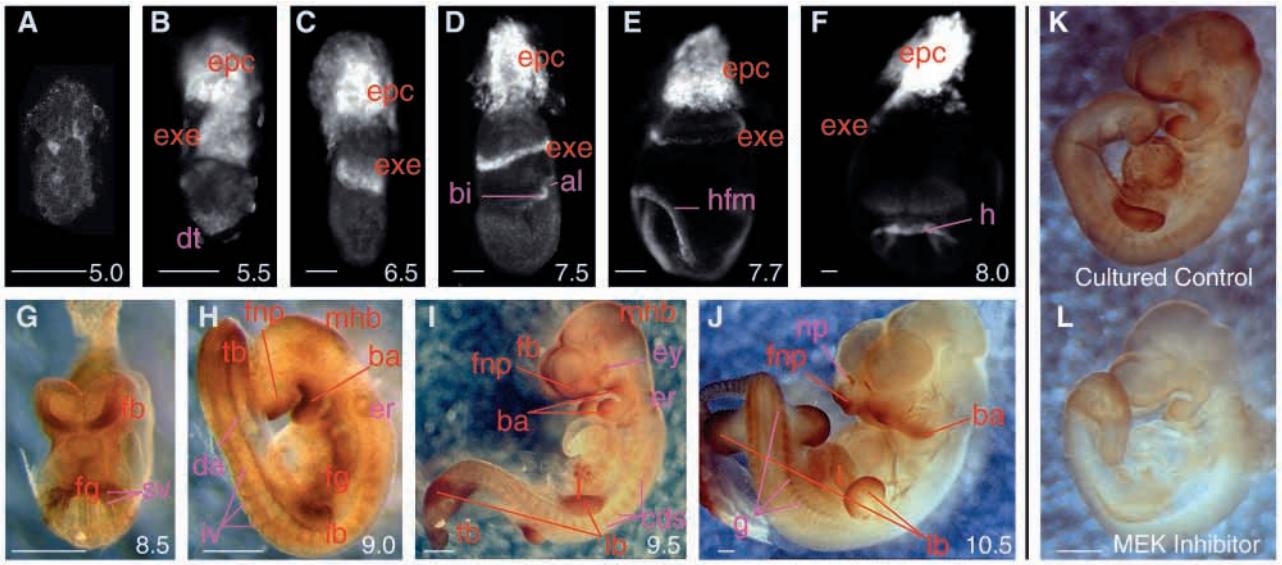

Fig. 1. Spatial and temporal patterns of phosphorylated ERK in postimplantation mouse embryos. (A-J) Embryos from indicated stages (5.0-10.5 dpc) were fixed and stained for dp-ERK immediately upon dissection to preserve endogeneous domains of signaling. (K,L) Embryos (9 dpc) were cultured in the absence (K) or presence (L) of 50 μM U0126 (MEK inhibitor) for 45 minutes prior to dp-ERK labeling to confirm staining was specific for the phosphorylated form of ERK. (A-F) Monochrome epifluorescence images of Cy3-dpERK labeled embryos. (G-L) DAB-HRP-dp-ERK stained embryos. Sustained ERK activation (color-coded with red lettering) is observed in the ectoplacental cone (epc), extra-embryonic ectoderm (exe), branchial arches (ba), frontonasal processes (fnp), tailbud (tb), limb buds (lb), forebrain (fb), midbrain-hindbrain boundary (mhb), foregut (fg) and liver primordia (l). Brief ERK activation (pink lettering) is seen in the distal tip of the epiblast (dt), allantoic bud (al), blood island mesoderm (bi), headfold mesoderm (hfm), heart primordia (h), sinus venosus (sv), dorsal aorta (da), intersomitic vessels (iv), eye primordia (ey), ear primordia (er), nasal pits (np), caudal region of somites (cds) and ganglia (g). Scale bars: ~50 μm in A-F; ~400 μm in G-L.

10.5+ dpc), liver primordia (9.5-10.5+ dpc), tailbud (8.5-10.5+ dpc) and placenta (8-10.5+ dpc) (Fig. 1G-J) (data not shown). ERK activation appeared in the limb bud field just prior to outgrowth (9 dpc), throughout the limb bud during early outgrowth (9-10 dpc), and in the distal region of later limb buds (10.5+ dpc). Signaling was sustained in the frontonasal process, the maxillary and mandibular components of the first branchial arches, and (to a lesser degree) in the second and third branchial arches during this period. In the CNS, dp-ERK staining was first observed in the neural ectoderm of the anterior forebrain and across the midbrain-hindbrain boundary at ~8.5-9.0 dpc (Fig. 1G) and later was most prominent in axons and nerve tracts in these regions (9-10.5+ dpc).

In addition to regions of sustained ERK signaling, brief and dynamic pulses of ERK activation were associated with blood vessel formation (8.0-10.5+ dpc), somite remodeling (~9.5 dpc), neural crest migration (9-9.5 dpc), as well as during development of the ear primordia (9-9.5 dpc), eye primordia (9-10.5+ dpc), nasal pits (10-10.5 dpc) and peripheral nervous system (10-10.5+ dpc). For example, at 8.5-9.0 dpc, dp-ERK was prevalent in the dorsal aorta (da) and then in the newly forming intersomitic vessels (iv) sprouting from the dorsal aorta (9 dpc) (Fig. 1H, Fig. 2A-E). At later stages (9.5-10.5+ dpc), dp-ERK staining in these established vessels was no longer detectable (Fig. 2F); only the most nascent blood vessels growing between the most caudal somites were dp-ERK positive (Fig. 1I,J, Fig. 2B-F). As a second example, at 9.0 dpc, dp-ERK was prevalent in neural crest cells migrating away

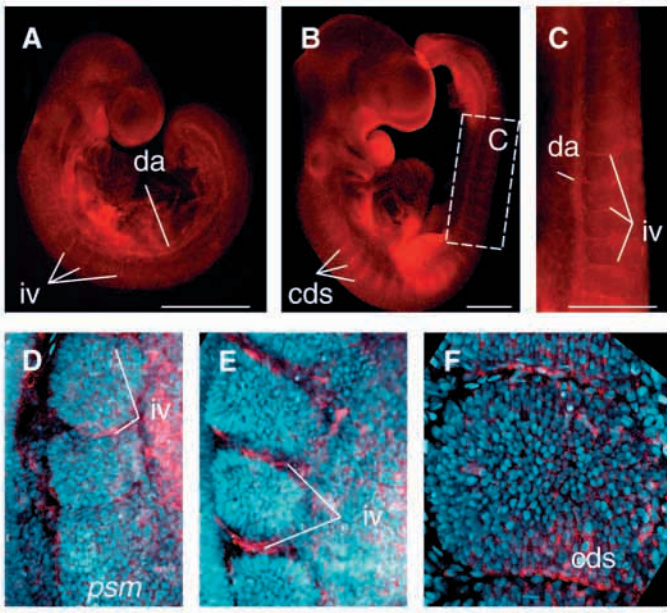

Fig. 2. Transient ERK signaling in intersomitic blood vessels. Low magnification view of Cy3-dpERK stained embryos at 9 dpc (A) and 9.5 dpc (B). (C) Higher magnification of region indicated in B. (D-F) Confocal composites of dp-ERK staining in somitic region at various stages of somite development. Dp-ERK staining is red. Nuclei (YOYO-1 staining) are shown in blue. Dp-ERK positive intersomitic vessels growing between newly formed somites are seen in D,E. In more mature blood vessels associated with more mature somites, dp-ERK staining is no longer associated with intersomitic vessels but rather with the caudal region of somites (B,F). da, dorsal aorta; iv, intersomitic vessels; cds, caudal portion of somite; psm, presomitic mesoderm. Scale bars: 500 μm.

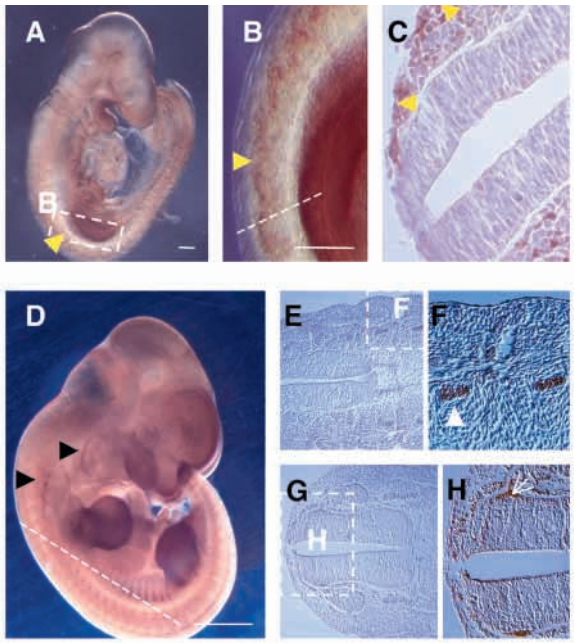

Fig. 3. ERK activation in peripheral nervous system. Dp-ERK stained 9.0 dpc (A) and 10.5 dpc (D) embryos with yellow arrowheads indicating neural crest and black arrowheads indicating nerve tracts of glossopharyngeal and vagus ganglia. Broken boxes approximate positions of the higher magnification panels indicated and broken lines in B and D approximate position of sections shown in C and E-H, respectively. White arrowhead (F) indicates dp-ERK positive dorsal root ganglia and white arrow (H) indicates dp-ERK staining in sensory nerve root found along the length of the neural tube at this stage. Scale bars: 600 μm.

from the neural tube (Fig. 3A-C) and then in newly formed ganglia and sensory nerve tracts at 10-10.5 dpc (Fig. 1J, Fig. 3D-H).

FGFR-dependent domains of ERK signaling

ERK has been implicated in multiple RTK signaling pathways, and many contiguous domains of ERK activation correlate with known or suspected regions of FGF signaling. The phenotypes of FGF and FGFR mutants have revealed roles of FGF signaling in limb bud outgrowth and patterning, craniofacial development, midbrain-hindbrain patterning, liver induction, placentation, and development of the eye and ear primordia (Faber et al., 2001; Goldfarb, 1996; Jung et al., 1999; Partanen et al., 1998; Szebenyi and Fallon, 1999; Trumpp et al., 1999; Xu et al., 1999).

In order to determine which dp-ERK positive domains were activated by FGF signaling, embryos were briefly cultured in an FGFR-specific inhibitor (SU5402) prior to staining. SU5402 binds the ATP binding site of FGFR receptors (Mohammadi et al., 1997) and is used widely in developmental systems to specifically block FGFR signaling (Maroon et al., 2002; Shinya et al., 2001). As seen in Fig. 4, dp-ERK staining was specifically diminished after SU5402 treatment in the extra-embryonic ectoderm (6-8 dpc), the heart primordia (8 dpc), limb buds, branchial arches, frontonasal process, midbrain-hindbrain boundary and eye primordia, implicating FGFR-dependent ERK signaling in these domains. By contrast, dp-

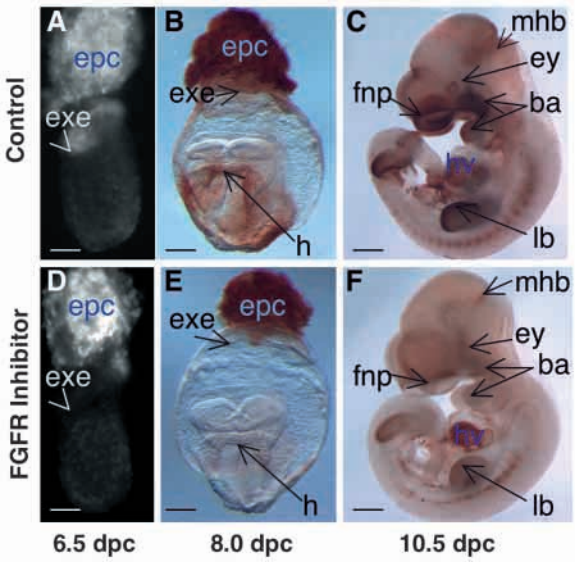

Fig. 4. FGFR-dependent ERK signaling in extra-embryonic ectoderm (exe), heart primordia (h), frontal nasal process (fnp), midbrain-hindbrain boundary (mhb), eye primordia (ey), branchial arches (ba) and limb buds (lb) at 6.5, 8.0 and 10.5 dpc. Prior to dp-ERK staining, embryos were cultured in the absence (A-C) or presence (D-F) of the FGFR inhibitor (40 μM SU5402) for 30-90 minutes. Note that culturing embryos alters dp-ERK patterns somewhat causing more diffuse boundaries of dp-ERK, some ectopic regions of dp-ERK and a loss of dp-ERK staining in some weaker regions of signaling. Dp-ERK staining in the ectoplacental cone (epc) and left heart ventricle (hv) were unaffected by the FGFR inhibitor. Scale bars: 50 μm in A,D; 100 μm in B,E; 700 μm in C,F.

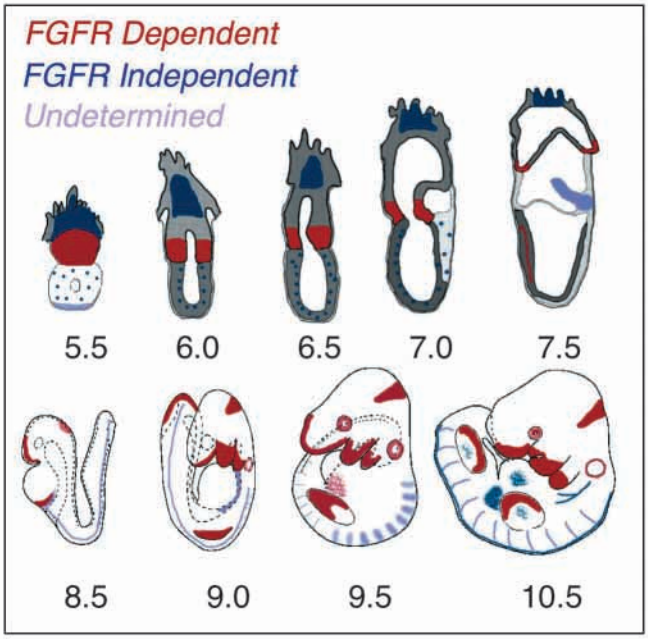

Fig. 5. Atlas of dp-ERK during mouse embryogenesis. Schematic overview of prominent ERK signaling domains during mouse development. Regions of FGFR signaling are colored red, non-FGFR signaling regions are blue and unclassified dp-ERK domains are purple. Note that regions of weak or transient ERK activation were not maintained in culture and thus no conclusion can be made about the effect of the FGFR inhibitor and hence the role of FGFR signaling in these domains. Diagrams of mouse embryos are adapted from http://genex.hgu.mrc.ac.uk

ERK staining in the EPC (Fig. 4D,E), mitotic cells of the embryo proper (Fig. 4D) and the heart ventricle (Fig. 4F) were unaffected by the inhibitor, suggesting other FGFR-independent signaling pathways are probably responsible for ERK activation in these regions. The inhibitor-treated embryos were always compared with cultured controls because culture, per se, altered dp-ERK patterns. Regions of transient, dynamic dp-ERK (such as blood vessels) rapidly lost dp-ERK staining after brief culture and could not be evaluated by these means.

Shown in Fig. 5 is a schematic summary of dp-ERK domains in postimplantation embryos with domains of FGFR-dependent ERK signaling colored red. FGFR-independent regions, which were unaffected by the FGFR inhibitor, are colored blue, and regions in which dp-ERK staining was lost rapidly upon embryo culture are colored purple. With the exception of the ectoplacental cone, all regions of sustained ERK signaling were FGFR dependent, including the extra-embryonic ectoderm, midbrain-hindbrain boundary, frontonasal process, branchial arches, tailbud and distal limb bud. Many regions of transient but strong dp-ERK staining were also FGFR dependent, including anlagen of the heart, eye and ear.

General characteristics of ERK signaling regions

Closer analysis of dp-ERK stained embryos revealed more details about the nature of ERK signaling in the mouse embryo. The most prominent dp-ERK staining was found in contiguous domains and appeared cytoplasmic. Shown in Fig. 6A-H is limb bud mesenchyme and forebrain neural ectoderm, but the same cytoplasmic staining was seen in all contiguous domains examined (Figs 2, 6-8 data not shown).

Mechanical injury also induced ERK activation in the mouse. As can be seen in Fig. 6I-L, random cells in the injured region of the embryo exhibited varying levels of both cytoplasmic and nuclear dp-ERK. From this, we concluded the absence of nuclear dp-ERK staining in the regions of endogeneous signaling (mentioned above) was not due to a technical problem with the staining procedure.

In addition to the contiguous domains of sustained ERK activation, dynamic, punctate staining was often observed, scattered throughout embryonic regions (e.g. Fig. 1A-D,G). Shown in Fig. 6M-P are dp-ERK positive cells along the apical side of the ectoderm of a gastrulating embryo (6.5 dpc). Double labeling embryos for dp-ERK and DNA revealed that over 85% of the apparently sporadic dp-ERK positive cells had condensed chromosomes, indicative of cells in mitosis. Only cells judged by chromosome morphology to be in prophase to early anaphase were dp-ERK positive, consistent with previous findings in cell culture in which ERK plays a role in entry into mitosis and exit from anaphase (Shapiro et al., 1998; Willard and Crouch, 2001).

FGFR-ERK signaling shaping the mouse embryo

Detailed analysis of the dp-ERK patterns that occur during the development of a tissue or organ can give insight into the

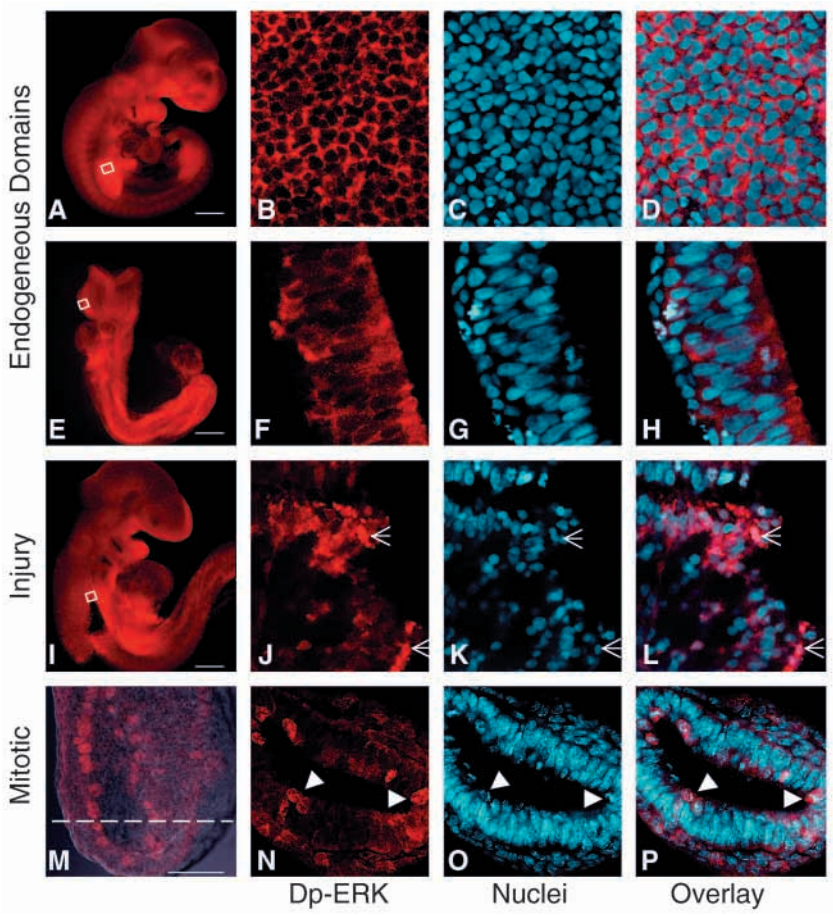

Fig. 6. Subcellular localization of activated ERK in mouse embryos. (A,E,I,M) Whole-mount views of dp-ERK stained embryos at 10.5, 8.5, 9.0 and 6.5 dpc, respectively. High magnification confocal and deconvolution sections of these dp-ERK stained embryos reveal cytoplasmic subcellular localization in endogeneous signaling domains such as limb bud mesenchyme (B-D) and forebrain neural ectoderm (F-H), but cytoplasmic and nuclear staining in mitotic cells (N-P) and regions of injury (J-L). (B-D,F-H,J-L) Confocal sections of dp-ERK/YOYO1 stained embryos in the regions indicated in A,E,I, respectively. (N-P) Deconvolution images of a dp-ERK/Hoechst-labeled embryo sectioned transversely at the position indicated in M. Arrowheads indicate mitotic dp-ERK positive cells. Arrows indicate non-mitotic cells that exhibit both cytoplasmic and nuclear dp-ERK staining in the region of torn somites. Scale bars: ~700 μm in A; ~250 μm in E; ~400 μm in I; ~75 μm in M.

signaling events shaping that tissue. In some cases, dp-ERK patterns corresponded to regions where FGF signaling is known to play specific roles. These patterns can be used to further our understanding of the signaling processes in such tissues.

Signaling in limb bud

In the limb bud, dp-ERK was first observed in the surface ectoderm during limb bud initiation (Fig. 7A). As limb bud outgrowth continued, dp-ERK diminished in the ectoderm and increased dramatically in the underlying mesenchyme (Fig. 7E). By the time the apical ectodermal ridge (AER) formed, a pronounced gradient of dp-ERK staining was seen in the mesenchymal (Fig. 7B-D) and ectodermal (Fig. 7F,G) cells with the intensity strongest adjacent to the AER, pointing to the AER as a putative FGF signaling source. In transverse sections, dp-ERK staining was observed in some regions of the dorsal and ventral surface ectoderm (Fig. 7F,G), suggesting there is FGF signaling from the underlying mesenchyme or perhaps autocrine signaling within the surface ectoderm. A gradient of dp-ERK was observed in the mesenchyme beneath the surface ectoderm in some regions (e.g. Fig. 7F ventral, Fig. 7G dorsal), indicating the surface ectoderm may also be a putative source of FGF signaling.

Genetic loss-of-function studies have evaluated the roles of FGF signaling in limb bud initiation, outgrowth and patterning in the proximodistal direction and have led to detailed models of FGF signaling in limb development (Martin, 1998) (depicted in Fig. 7H). FGF10 is thought to signal from the lateral plate mesoderm to FGFR2 in the overlying surface ectoderm to induce limb bud initiation (consistent with dp-ERK staining in the surface ectoderm in Fig. 7A,H). As outgrowth continues, FGF8 signals from the surface ectoderm to FGFR1 in the underlying mesenchyme (consistent with dp-ERK staining in Fig. 7E). By the time the AER forms, FGF4 and FGF8 are thought to signal to FGFR1 and FGFR2b in the progress zone mesenchyme beneath the AER (consistent with Fig. 7B-D,F,G).

Beyond just confirming current models of limb bud development with FGF signaling playing an important role in proximodistal outgrowth and patterning, the FGFR-dependent dp-ERK staining in the dorsal and ventral surface ectoderm and underlying mesenchyme (Fig. 7F,G) suggests FGF signaling may also play a role in dorsoventral patterning.

Signaling in the extra-embryonic ectoderm

The correlation between previously suspected regions of signaling and dp-ERK patterns in limb buds validated this approach of using phosphorylated ERK as a readout of the active signaling during mouse embryogenesis. There are many regions of FGFR-dependent dp-ERK staining, such as the extra-embryonic ectoderm, where the precise role of FGF has not yet been elucidated.

In the extra-embryonic ectoderm, *Fgfr2* is expressed throughout the entire Exe (as shown in Fig. 8I,J, depicted by yellow in Fig. 8F-H), but the FGFR-dependent dp-ERK staining was more restricted. ERK activation was first seen

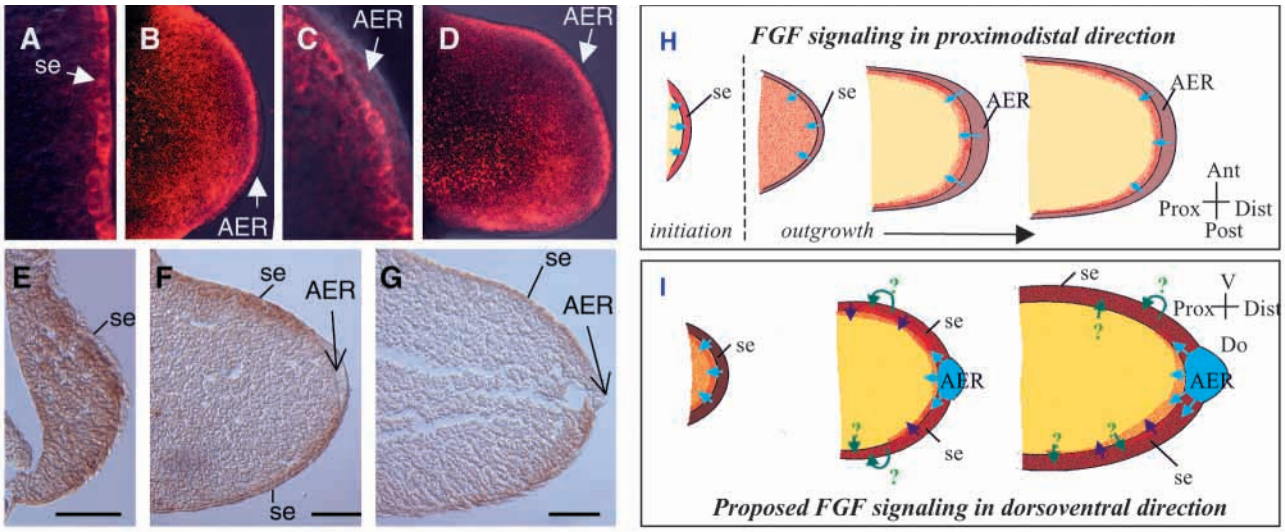

Fig. 7. FGFR-ERK signaling in limb buds. Dp-ERK staining in forelimb region at 9.0 dpc (A), 9.5 dpc (B,C) and 10.5 dpc (D). Initially, dp-ERK is detected in surface ectoderm (se) overlying lateral plate mesoderm (A). As limb bud outgrowth continues (B-D), a gradient of dp-ERK is seen in mesenchyme directly beneath the apical ectodermal ridge (AER). Transverse sections through hindlimbs at 9.5 dpc (E), 10.0 dpc (F) and 10.5 dpc (G). (H,I) Domains of FGF-dependent dp-ERK in developing limbs and proposed directions of FGF signaling shown with arrows. *Fgfr1* expression is shown in yellow, *Fgfr2* expression in brown and dp-ERK regions in red. Blue arrows indicate FGF signaling in the proximodistal directions, which is proposed by current models of limb development (Martin, 1998). Dp-ERK staining in the dorsal and ventral surface ectoderm suggest the possibility of mesenchyme to surface ectoderm FGF signaling or autocrine signaling within the surface ectoderm, as indicated by green arrows. Gradients of dp-ERK in mesenchyme beneath the surface ectoderm suggests FGF signaling from the surface ectoderm to mesenchyme (purple arrows). Scale bars: 50 μm.

throughout the entire Exe at ~5.5 dpc (Fig. 8A,F), after the initial formation of the tissue. The range of signaling gradually decreased as development continued and the domain of activation became restricted to a ring 6-9 cells across at 6.0 dpc (white bracket, Fig. 8B), 4-6 cells across at 7 dpc (white bracket, Fig. 8C) and only 2-4 cells across by 7.5 dpc (white bracket, Fig. 8D). At the early stages, a gradient of dp-ERK with strongest staining in the proximal Exe was observed (Fig. 8A,B), suggesting that the receptor is activated by FGFs, possibly FGF4 (Niswander and Martin, 1992), derived from the adjacent epiblast. By later stages (7-8 dpc), the gradient of dp-ERK had disappeared and the distal boundary of ERK activation was sharp (Fig. 8C-E,H). In these older embryos (7-8 dpc), dp-ERK staining was seen in both the peripheral and internal layers of the extraembryonic ectoderm (Fig. 8E), suggesting extra-embryonic mesoderm cells at the base of the chorion are the likely source of FGF (see Fig. 8H).

FGF-dependent trophoblast stem cells (TS cells) have

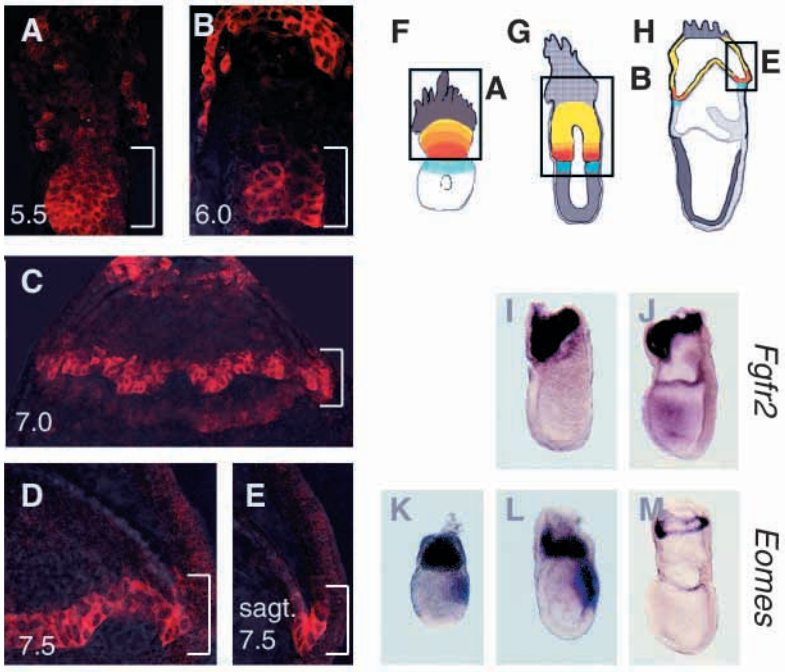

Fig. 8. FGFR-ERK signaling in extra-embryonic ectoderm. Confocal images (400×) of dp-ERK stained embryos superimposed on DIC images at (A) 5.5 dpc, (B) 6.0 dpc, (C) 7.0 dpc and (D-E) 7.5 dpc. The entire extra-embryonic region is shown in A,B whereas the EPC has been removed in C-E. White brackets indicate extent of dp-ERK staining in extra-embryonic ectoderm. (E) Sagittal section of D showing dp-ERK in both the internal and peripheral layers of the extra-embryonic ectoderm. (F-H) Schematic diagram depicting the *Fgfr2*-expressing extra-embryonic ectoderm in yellow, the domains of dp-ERK in the extra-embryonic ectoderm in red and the location of the proposed FGF signaling sources in blue. Boxes in F-H demarcate the region of embryo shown in confocal images (A,B,E). Initially, a gradient of dp-ERK can be seen throughout the entire extra-embryonic ectoderm at ~5.5 dpc (A,F). This gradient becomes reduced and spans a distance of six to nine cell diameters by ~6.0 (B,G). The upper boundary sharpens and the band of dp-ERK is reduced to four to six cell-diameters by 7.0 (C) and to two to four cell-diameters by 7.5 dpc (D,H). In situs show expression pattern of *Fgfr2* throughout the extra-embryonic ectoderm at 6.5 (I) and 7.5 dpc (J). In situs of *Eomes* at 5.5 (K), 6.5 (L) and 7.5 dpc (M) correspond closely to regions of ERK activation. (I-M) Adapted, with permission, from Ciruna and Rossant (Ciruna and Rossant, 1999).

been derived from the Exe at the stages the FGFR-dependent dp-ERK ring is evident (6-8 dpc) (Tanaka et al., 1998; Uy et al., 2002). Tanaka et al. proposed a model in which FGF4 signals from the epiblast to the overlaying *Fgfr2*-expressing Exe to sustain this stem cell population in vivo (Tanaka et al., 1998). The staining pattern is consistent with this and, thus, the dp-ERK ring may demarcate the stem cell population in vivo.

Discussion

Dp-ERK domains reveal spatial and temporal patterns of signaling during mouse embryogenesis

In these studies, we follow the active state of RTK-ERK signaling pathways in situ using antibodies specific for the active, diphosphorylated form of ERK. Prominent, sustained ERK activation was observed in the ectoplacental cone, extra-embryonic ectoderm, midbrain-hindbrain boundary, forebrain, frontonasal process, branchial arches, limb buds, foregut and liver, implicating sustained RTK-ERK signaling in these regions. By contrast, brief pulses of ERK activation were seen in the distal tip of the pregastrulation epiblast, the allantoic bud, headfold mesoderm, heart primordia, somites, peripheral neurons, and anlagen of the eye and ear, suggesting RTK-ERK signaling plays a more transient, dynamic role in these structures.

Detailed analysis of the spatial and temporal pattern of dp-ERK within a given tissue yielded further insights into the specific role of RTK-ERK signaling in the region. In the limb buds, dp-ERK patterns were consistent with previously identified roles of FGF signaling from the lateral plate mesoderm to surface ectoderm (in order to induce limb bud initiation), from surface ectoderm to underlying mesenchyme (in order to stimulate outgrowth) and from AER to underlying mesenchyme (to promote proliferation, outgrowth, cell survival and patterning) (Fig. 7).

The parallels between dp-ERK patterns and current models of FGF signaling in the limb bud validated this approach as a means to visualize signaling processes and permit speculation on the roles of signaling in various, less well studied regions. For example, in blood vessels, dp-ERK was seen transiently in newly forming vessels but was attenuated as vessels matured, suggesting a role of ERK signaling in blood vessel establishment but not maintenance. Consistent with this, mutations in the *Flk1* receptor prevent blood vessel formation (Shalaby et al., 1995), suggesting the transient ERK activation in nascent blood vessels may be due to FLK1-ERK signaling. A brief pulse of FGFR-dependent ERK activation in the heart primordia (Fig. 1F; Fig. 4B,E) indicated FGF signaling may play a role in heart induction in mouse as it does in zebrafish and chicken (Alsan and Schultheiss, 2002; Reifers et al., 2000). In the EPC, dp-ERK staining began after the initial formation of the tissue and persisted for several days in the central diploid cells (Fig. 1) suggesting a continued role of ERK signaling in the maintenance, patterning and/or proliferation of the region. Similarly, patterns of ERK activation associated with structures such as the eye, ear, branchial arches, extra-embryonic ectoderm and peripheral nervous system provide insight into precisely when and where signaling occurs during the genesis of these tissues.

Most dp-ERK domains correspond to regions of FGF signaling in mouse

With more than 50 different RTKs in mouse and potential crosstalk with other signaling pathways, it is striking that domains of dp-ERK were so discrete. Many domains of dp-ERK correspond to regions of known or speculated FGF signaling in mouse, and dp-ERK staining was abolished or attenuated in most domains by an FGFR-specific inhibitor (Figs 4, 5). The majority of dp-ERK domains in *Xenopus* and zebrafish are also FGFR-dependent (Christen and Slack, 1999; Curran and Grainger, 2000; Shinya et al., 2001), and FGFs induce particularly robust and sustained MAPK responses in cell culture (Hadari et al., 1998; Marshall, 1995). Although RAS-ERK was described initially as a universal signaling cascade downstream of all RTKs, some RTKs elicit only weak RAS-ERK responses, preferentially use other pathways or even inhibit the RAS-ERK cascade (Elowe et al., 2001; Schlessinger, 2000). Thus, not all domains of RTK signaling are scored in this assay. Instead, dp-ERK staining in mouse embryos primarily reveals FGF signaling domains.

Although the majority of dp-ERK domains were FGFR dependent, not all domains of FGFR signaling were dp-ERK positive. Loss-of-function studies reveal FGFR1 is essential for mesoderm migration through the primitive streak and somite formation (Ciruna et al., 1997; Deng et al., 1994; Yamaguchi et al., 1994). Yet detailed examination of various stages failed to reveal significant dp-ERK staining in these regions aside from sporadic mitotic cells (see Fig. 6M-P, Fig. 2D). This lack of dp-ERK staining was surprising as FGFR-dependent ERK signaling is prominent in the primitive streak of *Xenopus* and zebrafish embryos (Christen and Slack, 1999; Curran and Grainger, 2000; Shinya et al., 2001), as well as in the newly forming somites of zebrafish (Sawada et al., 2001). However, weak dp-ERK staining was occasionally seen in newly forming somites (in two embryos out of ~80), suggesting transient FGFR1-ERK signaling may occur in this region. Negative feedback inhibitors of the FGFR-ERK signaling pathway, including Sprouty genes, *Sef* and MAP kinase phosphatase genes, are highly expressed in these regions of the embryo (Dickinson et al., 2002a; Klock and Herrmann, 2002; Lin et al., 2002; Minowada et al., 1999) and may account for decreased dp-ERK staining. Alternatively, FGFR1 may signal preferentially through another pathway (such as PI3 kinase, PLCγ or perhaps other MAPKs) in these tissues.

Not all dp-ERK domains were eliminated by treatment with an FGFR inhibitor. These FGFR-independent domains, including the EPC and sensory neurons, are probably due to other signaling pathways that must also lead to sustained ERK activation. Neurotrophins signaling through TRK receptors are essential for sensory neuron survival, outgrowth and differentiation, and are likely candidates for ERK signaling in nerve tracts and ganglia of the peripheral nervous system (Crowley et al., 1994; Farinas et al., 2002; Smeyne et al., 1994). EGF or HGF signaling may be responsible for dp-ERK staining in the EPC (Patel et al., 2000; Sibilia and Wagner, 1995).

Dp-ERK domains define regions where target genes of the signaling pathways can be sought

The dp-ERK positive cells in a given region likely receive patterning and differentiation cues that are different from those

in adjacent dp-ERK negative cells. Thus, spatial and temporal correlation of gene expression with a dp-ERK domain indicates that the gene may be a downstream target of the signaling pathway.

Previous studies have shown *Lhx6* and *Evx1* to be downstream of FGF signaling in the branchial arch and limb, respectively (Niswander and Martin, 1993; Trumpp et al., 1999), and indeed expression patterns of these genes closely correlate with the FGFR-dependent dp-ERK patterns. In the Exe, it is striking that expression of trophoblast stem cell genes *Eomes* and *Sox2* are expressed in essentially identical spatial and temporal patterns as dp-ERK (see Fig. 8) (Ciruna and Rossant, 1999; Wood and Episkopou, 1999), suggesting they are downstream targets of FGF signaling in the Exe. Additional studies are needed to test the relationship between FGF signaling and expression of *Eomes* and *Sox2*. However, other T-box and HMG transcription factors are known to be downstream of FGF signaling in other tissues (Faber et al., 2001; LaBonne et al., 1995; Murakami et al., 2000; Smith et al., 1991). These genes, as well as additional unknown genes sharing similar spatial and temporal expression patterns, are excellent candidate targets of FGF signaling in the region.

Dp-ERK domains give insight into properties of ERK signaling in vivo

From analysis of the spatial and temporal patterns of ERK activation, we have gained insight into signaling processes as they occur in the three-dimensional context of the mouse embryo.

Gradients versus sharp boundaries

During development, highly regulated growth factor signaling is known to pattern fields of cells. Such signaling is not solely controlled by availability of growth factor. A parallel set of inhibitory mechanisms is often used to spatially and temporally restrict levels of signaling. In the Exe, a gradient of FGFR-dependent ERK activation was seen throughout the tissues at 5.5 dpc, gradually diminished in intensity (Fig. 1B-F), and became restricted to a ring two cells in diameter by 7.5 dpc (Fig. 8D). FGFR inhibitors, *Sef* and *Sprouty* genes, are induced by FGF signaling (Chambers et al., 2000; Furthauer et al., 2002; Ozaki et al., 2001), and are expressed in patterns consistent with a role in shaping the boundaries of this dp-ERK domain in the Exe. *Sef* is expressed in a gradient from the distal to proximal Exe (Lin et al., 2002), indicating it may play a role to attenuate signaling in the distal Exe. *Spry2*, however, is transcriptionally induced in the same region where dp-ERK is evident (Minowada et al., 1999) and may play a cell-autonomous role in modulating the ERK response over time (Tefft et al., 2002). Sprouty genes and *Sef* are also expressed in the limb bud and probably play a role in modulating ERK signaling in the region. Additional studies will be needed to compare precisely domains of inhibitor expression with dp-ERK staining and to test the role of inhibitors functionally in defining boundaries (and intensities) of dp-ERK domains.

Signaling through cytoplasmic ERK

Although many aspects of ERK signaling in mouse were consistent with findings in *Drosophila*, *Xenopus* and zebrafish, one striking difference did exist: phosphorylated ERK appeared predominantly cytoplasmic in the contiguous dp-ERK domains of the mouse, whereas dp-ERK is nuclear in *Drosophila* and Xenopus embryos (Curran and Grainger, 2000; Gabay et al., 1997a; Gabay et al., 1997b). It seems unlikely that there was a technical problem with nuclear dp-ERK detection in the mouse embryos because nuclear dp-ERK was easily observed in regions of injury (Fig. 6).

One explanation for the apparent discrepancy is that the nuclear localization of ERK may be transient in the mouse embryo. Phosphorylated ERK may shuttle to the nucleus upon initial activation of the signaling pathway but rapidly be dephosphorylated by nuclear MAPK phosphatases (MKP1 and MKP2) (Volmat et al., 2001) or become exported from the nucleus, such that only cytoplasmic dp-ERK is detected. Confocal sectioning through the entire dp-ERK regions, in which signaling was just beginning (such as the Exe at 5-5.5 dpc), however, failed to reveal any evidence for nuclear dp-ERK. Furthermore, when we analyzed the FGF-ERK signaling cascade in trophoblast stem cells derived from the Exe (Tanaka et al., 1998), only sustained cytoplasmic dp-ERK was detected in cell culture (L.B.C. and J.R., unpublished). Taken together, this suggests phosphorylated ERK may not translocate to the nucleus in endogenous domains of sustained signaling in mouse embryos.

Biochemical analysis of the RAS-ERK signaling cascade in cell culture has lead to current models of ERK-mediated transcription in which nuclear translocation of phosphorylated ERK is important for activation of various transcription factors (Pouyssegur et al., 2002). However, ERK has numerous targets in the cytoplasm, cytoskeleton and plasma membrane (Pearson et al., 2001). Cytoplasmic ERK may mediate a transcriptional response in the mouse by phosphorylating cytosolic proteins involved in transcriptional regulation, such as $p90^{RSK}$, which in turn relay signals to the nucleus. Sprouty and MAP kinase phosphatase genes are transcriptionally induced by ERK (Camps et al., 1998; Chambers et al., 2000; Ozaki et al., 2001) and exhibit expression patterns correlating with subsets of dp-ERK domains (Dickinson et al., 2002a; Dickinson et al., 2002b; Minowada et al., 1999). Thus, there is evidence for ERK-mediated transcription in regions where only cytoplasmic dp-ERK is detected. Of interest, this co-localization of the negative feedback inhibitors with dp-ERK domains provides a means to control the duration and magnitude of MAPK activation in each region, which is a parameter shown to be crucial for cell fate decisions (Marshall, 1995).

Cytoplasmic ERK also participates in the regulation of cytoskeletal architecture in a manner that is independent of transcriptional regulation. ERK has been implicated in cytoskeletal remodeling and focal adhesion assembly required in cell motility (Fincham et al., 2000; Klemke et al., 1997). Thus, cytoplasmic dp-ERK in sprouting blood vessels, migrating neural crest and outgrowing sensory axons may be sufficient for the roles of ERK in these cell populations.

In summary, this atlas of dp-ERK domains provides an overview of active ERK signaling regions in the mouse embryo. The timing, location, intensity, duration and magnitude of ERK activation in various regions yields insight into how signaling is shaping the mouse embryo, how this signaling is regulated in vivo, and where to look for downstream targets of the signaling cascades.

We thank the SLRI mouse facility (especially J. Cabezas) for providing timed pregnant female mice, and K. Harpel and B. Ciruna for embryo sectioning, M. Woodside at the Hospital for Sick Children's Imaging Center for assistance with confocal imaging. We thank members of the Rossant and Pawson laboratories (especially S. H. Ong, S. Elowe, A. Pawson, B. Ciruna, C. Chazaud, D. Strumpf and M. Ema) for insightful discussion. This work was funded by CIHR grants to J.R. J.R. is a CIHR Distinguished Investigator. L.B.C. is the recipient of a Canadian MRC Postdoctoral Fellowship (2000) and a Human Frontier Scientific Organization Long Term Postdoctoral Fellowship (2001-present). The Imaging Center at the Hospital for Sick Children in Toronto is funded by a CIHR maintenance grant.

References

Alsan, B. H. and Schultheiss, T. M. (2002). Regulation of avian cardiogenesis by Fgf8 signaling. *Development* **129**, 1935-1943.

Belcheva, M. M. and Coscia, C. J. (2002). Diversity of G protein-coupled receptor signaling pathways to ERK/MAP kinase. *Neurosignals* **11**, 34-44.

Camps, M., Chabert, C., Muda, M., Boschert, U., Gillieron, C. and Arkinstall, S. (1998). Induction of the mitogen-activated protein kinase phosphatase MKP3 by nerve growth factor in differentiating PC12. *FEBS Lett.* **425**, 271-276.

Chambers, D., Medhurst, A. D., Walsh, F. S., Price, J. and Mason, I. (2000). Differential display of genes expressed at the midbrain – hindbrain junction identifies sprouty2: an FGF8-inducible member of a family of intracellular FGF antagonists. *Mol. Cell Neurosci.* **15**, 22-35.

Christen, B. and Slack, J. M. (1999). Spatial response to fibroblast growth factor signalling in Xenopus embryos. *Development* **126**, 119-125.

Ciruna, B. G. and Rossant, J. (1999). Expression of the T-box gene Eomesodermin during early mouse development. *Mech. Dev.* **81**, 199-203.

Ciruna, B. G., Schwartz, L., Harpal, K., Yamaguchi, T. P. and Rossant, J. (1997). Chimeric analysis of fibroblast growth factor receptor-1 (Fgfr1) function: a role for FGFR1 in morphogenetic movement through the primitive streak. *Development* **124**, 2829-2841.

Crowley, C., Spencer, S. D., Nishimura, M. C., Chen, K. S., Pitts-Meek, S., Armanini, M. P., Ling, L. H., MacMahon, S. B., Shelton, D. L., Levinson, A. D. et al. (1994). Mice lacking nerve growth factor display perinatal loss of sensory and sympathetic neurons yet develop basal forebrain cholinergic neurons. *Cell* **76**, 1001-1011.

Curran, K. L. and Grainger, R. M. (2000). Expression of activated MAP kinase in Xenopus laevis embryos: evaluating the roles of FGF and other signaling pathways in early induction and patterning. *Dev. Biol.* **228**, 41-56.

Deng, C. X., Wynshaw-Boris, A., Shen, M. M., Daugherty, C., Ornitz, D. M. and Leder, P. (1994). Murine FGFR-1 is required for early postimplantation growth and axial organization. *Genes Dev.* **8**, 3045-3057.

Dickinson, R. J., Eblaghie, M. C., Keyse, S. M. and Morriss-Kay, G. M. (2002a). Expression of the ERK-specific MAP kinase phosphatase PYST1/MKP3 in mouse embryos during morphogenesis and early organogenesis. *Mech. Dev.* **113**, 193-196.

Dickinson, R. J., Williams, D. J., Slack, D. N., Williamson, J., Seternes, O. M. and Keyse, S. M. (2002b). Characterization of a murine gene encoding a developmentally regulated cytoplasmic dual-specificity mitogen-activated protein kinase phosphatase. *Biochem. J.* **364**, 145-155.

Elowe, S., Holland, S. J., Kulkarni, S. and Pawson, T. (2001). Downregulation of the Ras-mitogen-activated protein kinase pathway by the EphB2 receptor tyrosine kinase is required for ephrin-induced neurite retraction. *Mol. Cell. Biol.* **21**, 7429-7441.

Faber, S. C., Dimanlig, P., Makarenkova, H. P., Shirke, S., Ko, K. and Lang, R. A. (2001). Fgf receptor signaling plays a role in lens induction. *Development* **128**, 4425-4438.

Farinas, I., Cano-Jaimez, M., Bellmunt, E. and Soriano, M. (2002). Regulation of neurogenesis by neurotrophins in developing spinal sensory ganglia. *Brain Res. Bull.* **57**, 809-816.

Feldmann, P., Eicher, E. N., Leevers, S. J., Hafen, E. and Hughes, D. A. (1999). Control of growth and differentiation by Drosophila RasGAP, a homolog of p120 Ras-GTPase-activating protein. *Mol. Cell. Biol.* **19**, 1928-1937.

Fincham, V. J., James, M., Frame, M. C. and Winder, S. J. (2000). Active ERK/MAP kinase is targeted to newly forming cell-matrix adhesions by integrin engagement and v-Src. *EMBO J.* **19**, 2911-2923.

Furthauer, M., Lin, W., Ang, S. L., Thisse, B. and Thisse, C. (2002). Sef is a feedback-induced antagonist of Ras/MAPK-mediated FGF signalling. *Nat. Cell Biol.* **4**, 170-174.

Gabay, L., Seger, R. and Shilo, B. Z. (1997a). In situ activation pattern of Drosophila EGF receptor pathway during development. *Science* **277**, 1103-1106.

Gabay, L., Seger, R. and Shilo, B. Z. (1997b). MAP kinase in situ activation atlas during Drosophila embryogenesis. *Development* **124**, 3535-3541.

Goldfarb, M. (1996). Functions of fibroblast growth factors in vertebrate development. *Cytokine Growth Factor Rev.* **7**, 311-325.

Hadari, Y. R., Kouhara, H., Lax, I. and Schlessinger, J. (1998). Binding of Shp2 tyrosine phosphatase to FRS2 is essential for fibroblast growth factor-induced PC12 cell differentiation. *Mol. Cell. Biol.* **18**, 3966-3973.

Jung, J., Zheng, M., Goldfarb, M. and Zaret, K. S. (1999). Initiation of mammalian liver development from endoderm by fibroblast growth factors. *Science* **284**, 1998-2003.

Klemke, R. L., Cai, S., Giannini, A. L., Gallagher, P. J., de Lanerolle, P. and Cheresh, D. A. (1997). Regulation of cell motility by mitogen-activated protein kinase. *J. Cell Biol.* **137**, 481-492.

Klock, A. and Herrmann, B. G. (2002). Cloning and expression of the mouse dual-specificity mitogen-activated protein (MAP) kinase phosphatase Mkp3 during mouse embryogenesis. *Mech. Dev.* **116**, 243-247.

LaBonne, C., Burke, B. and Whitman, M. (1995). Role of MAP kinase in mesoderm induction and axial patterning during Xenopus development. *Development* **121**, 1475-1486.

Lai, K. M. and Pawson, T. (2000). The ShcA phosphotyrosine docking protein sensitizes cardiovascular signaling in the mouse embryo. *Genes Dev.* **14**, 1132-1145.

Lin, W., Furthauer, M., Thisse, B., Thisse, C., Jing, N. and Ang, S. L. (2002). Cloning of the mouse Sef gene and comparative analysis of its expression with Fgf8 and Spry2 during embryogenesis. *Mech. Dev.* **113**, 163-168.

Maroon, H., Walshe, J., Mahmood, R., Kiefer, P., Dickson, C. and Mason, I. (2002). Fgf3 and Fgf8 are required together for formation of the otic placode and vesicle. *Development* **129**, 2099-2108.

Marshall, C. J. (1995). Specificity of receptor tyrosine kinase signaling: transient versus sustained extracellular signal-regulated kinase activation. *Cell* **80**, 179-185.

Martin, G. R. (1998). The roles of FGFs in the early development of vertebrate limbs. *Genes Dev.* **12**, 1571-1586.

Minowada, G., Jarvis, L. A., Chi, C. L., Neubuser, A., Sun, X., Hacohen, N., Krasnow, M. A. and Martin, G. R. (1999). Vertebrate Sprouty genes are induced by FGF signaling and can cause chondrodysplasia when overexpressed. *Development* **126**, 4465-4475.

Mohammadi, M., McMahon, G., Sun, L., Tang, C., Hirth, P., Yeh, B. K., Hubbard, S. R. and Schlessinger, J. (1997). Structures of the tyrosine kinase domain of fibroblast growth factor receptor in complex with inhibitors. *Science* **276**, 955-960.

Murakami, S., Kan, M., McKeehan, W. L. and de Crombrugghe, B. (2000). Up-regulation of the chondrogenic Sox9 gene by fibroblast growth factors is mediated by the mitogen-activated protein kinase pathway. *Proc. Natl. Acad. Sci. USA* **97**, 1113-1118.

Niswander, L. and Martin, G. R. (1992). Fgf-4 expression during gastrulation, myogenesis, limb and tooth development in the mouse. *Development* **114**, 755-768.

Niswander, L. and Martin, G. R. (1993). FGF-4 regulates expression of Evx-1 in the developing mouse limb. *Development* **119**, 287-294.

Ozaki, K., Kadomoto, R., Asato, K., Tanimura, S., Itoh, N. and Kohno, M. (2001). ERK pathway positively regulates the expression of Sprouty genes. *Biochem. Biophys. Res. Commun.* **285**, 1084-1088.

Partanen, J., Schwartz, L. and Rossant, J. (1998). Opposite phenotypes of hypomorphic and Y766 phosphorylation site mutations reveal a function for Fgfr1 in anteroposterior patterning of mouse embryos. *Genes Dev.* **12**, 2332-2344.

Patel, Y., Kim, H. and Rappolee, D. A. (2000). A role for hepatocyte growth factor during early postimplantation growth of the placental lineage in mice. *Biol. Reprod.* **62**, 904-912.

Pearson, G., Robinson, F., Beers Gibson, T., Xu, B. E., Karandikar, M., Berman, K. and Cobb, M. H. (2001). Mitogen-activated protein (MAP) kinase pathways: regulation and physiological functions. *Endocr. Rev.* **22**, 153-183.

Pouyssegur, J., Volmat, V. and Lenormand, P. (2002). Fidelity and spatio-temporal control in MAP kinase (ERKs) signalling. *Biochem. Pharmacol.* **64**, 755-763.

Reich, A., Sapir, A. and Shilo, B. (1999). Sprouty is a general inhibitor of receptor tyrosine kinase signaling. *Development* **126**, 4139-4147.

Reifers, F., Walsh, E. C., Leger, S., Stainier, D. Y. and Brand, M. (2000). Induction and differentiation of the zebrafish heart requires fibroblast growth factor 8 (fgf8/acerebellar). *Development* **127**, 225-235.

Sawada, A., Shinya, M., Jiang, Y. J., Kawakami, A., Kuroiwa, A. and Takeda, H. (2001). Fgf/MAPK signalling is a crucial positional cue in somite boundary formation. *Development* **128**, 4873-4880.

Schlessinger, J. (2000). Cell signaling by receptor tyrosine kinases. *Cell* **103**, 211-225.

Shalaby, F., Rossant, J., Yamaguchi, T. P., Gertsenstein, M., Wu, X. F., Breitman, M. L. and Schuh, A. C. (1995). Failure of blood-island formation and vasculogenesis in Flk-1-deficient mice. *Nature* **376**, 62-66.

Shapiro, P. S., Vaisberg, E., Hunt, A. J., Tolwinski, N. S., Whalen, A. M., McIntosh, J. R. and Ahn, N. G. (1998). Activation of the MKK/ERK pathway during somatic cell mitosis: direct interactions of active ERK with kinetochores and regulation of the mitotic 3F3/2 phosphoantigen. *J. Cell Biol.* **142**, 1533-1545.

Shinya, M., Koshida, S., Sawada, A., Kuroiwa, A. and Takeda, H. (2001). Fgf signalling through MAPK cascade is required for development of the subpallial telencephalon in zebrafish embryos. *Development* **128**, 4153-4164.

Sibilia, M. and Wagner, E. F. (1995). Strain-dependent epithelial defects in mice lacking the EGF receptor. *Science* **269**, 234-238.

Smeyne, R. J., Klein, R., Schnapp, A., Long, L. K., Bryant, S., Lewin, A., Lira, S. A. and Barbacid, M. (1994). Severe sensory and sympathetic neuropathies in mice carrying a disrupted Trk/NGF receptor gene. *Nature* **368**, 246-249.

Smith, J. C., Price, B. M., Green, J. B., Weigel, D. and Herrmann, B. G. (1991). Expression of a Xenopus homolog of Brachyury (T) is an immediate-early response to mesoderm induction. *Cell* **67**, 79-87.

Szebenyi, G. and Fallon, J. F. (1999). Fibroblast growth factors as multifunctional signaling factors. *Int. Rev. Cytol.* **185**, 45-106.

Tanaka, S., Kunath, T., Hadjantonakis, A. K., Nagy, A. and Rossant, J. (1998). Promotion of trophoblast stem cell proliferation by FGF4. *Science* **282**, 2072-2075.

Tefft, D., Lee, M., Smith, S., Crowe, D. L., Bellusci, S. and Warburton, D. (2002). mSprouty2 inhibits FGF10-activated MAP kinase by differentially binding to upstream target proteins. *Am. J. Physiol. Lung. Cell Mol. Physiol.* **283**, L700-L706.

Trumpp, A., Depew, M. J., Rubenstein, J. L., Bishop, J. M. and Martin, G. R. (1999). Cre-mediated gene inactivation demonstrates that FGF8 is required for cell survival and patterning of the first branchial arch. *Genes Dev.* **13**, 3136-3148.

Uy, G. D., Downs, K. M. and Gardner, R. L. (2002). Inhibition of trophoblast stem cell potential in chorionic ectoderm coincides with occlusion of the ectoplacental cavity in the mouse. *Development* **129**, 3913-3924.

Volmat, V., Camps, M., Arkinstall, S., Pouyssegur, J. and Lenormand, P. (2001). The nucleus, a site for signal termination by sequestration and inactivation of p42/p44 MAP kinases. *J. Cell Sci.* **114**, 3433-3443.

Wakioka, T., Sasaki, A., Kato, R., Shouda, T., Matsumoto, A., Miyoshi, K., Tsuneoka, M., Komiya, S., Baron, R. and Yoshimura, A. (2001). Spred is a Sprouty-related suppressor of Ras signalling. *Nature* **412**, 647-651.

Widmann, C., Gibson, S., Jarpe, M. B. and Johnson, G. L. (1999). Mitogen-activated protein kinase: conservation of a three-kinase module from yeast to human. *Physiol. Rev.* **79**, 143-180.

Willard, F. S. and Crouch, M. F. (2001). MEK, ERK, and p90RSK are present on mitotic tubulin in Swiss 3T3 cells: a role for the MAP kinase pathway in regulating mitotic exit. *Cell Signal* **13**, 653-664.

Wood, H. B. and Episkopou, V. (1999). Comparative expression of the mouse Sox1, Sox2 and Sox3 genes from pre- gastrulation to early somite stages. *Mech. Dev.* **86**, 197-201.

Xu, X., Weinstein, M., Li, C. and Deng, C. (1999). Fibroblast growth factor receptors (FGFRs) and their roles in limb development. *Cell Tissue Res.* **296**, 33-43.

Yamaguchi, T. P., Harpal, K., Henkemeyer, M. and Rossant, J. (1994). fgfr-1 is required for embryonic growth and mesodermal patterning during mouse gastrulation. *Genes Dev.* **8**, 3032-3044.